


Emittance growth analysis of laser-driven broad energy spectral proton beams

M. J. Wu¹, D. Y. Li, T. Yang², Y. Z. Li, H. Cheng, Y. D. Xia, Y. Yan, Y. L. Fang, K. Zhu, M. J. Easton³, C. Lin,^{*} and X. Q. Yan

State Key Laboratory of Nuclear Physics and Technology, and Key Laboratory of HEDP of the Ministry of Education, CAPT, Peking University, Beijing 100871, China

 (Received 1 August 2023; accepted 1 April 2024; published 22 April 2024)

With the rapid development of high-gradient laser plasma acceleration, implementing it in practical applications has become a priority. However, to go from “acceleration” to “accelerator,” a beam line system is required to accurately control the beam parameters according to different irradiation requirements. The laser-accelerated proton beam is characterized by a micron-scale original source size and a small emittance as low as 0.004 mm mrad [T. E. Cowan *et al.*, *Phys. Rev. Lett.* **92**, 204801 (2004)]. However, due to the broad energy spread and large divergence, its initial ultralow emittance will increase rapidly in the subsequent transmission process. This indicates that designing a beamline for laser-driven protons is challenging and differs significantly from that of a conventional accelerator. As a fundamental parameter for beam line design, we have theoretically derived the emittance growth law for laser-driven protons in both drift space and in a focusing element. The results demonstrate that the beam emittance deteriorates sharply with the energy spread and the square of the divergence angle. These theoretical calculations have been verified both in experiments and simulations. This work is helpful for designing subsequent beam lines that pursue high transmission efficiency and achromatic ability.

DOI: [10.1103/PhysRevAccelBeams.27.041303](https://doi.org/10.1103/PhysRevAccelBeams.27.041303)

I. INTRODUCTION

Laser plasma acceleration has attracted a great deal of attention due to its high accelerated field (10^{12} V/m) [1]. Recently, the energy of protons accelerated by ultrahigh-intensity laser pulses irradiating solid ultrathin (90 nm) targets has reached 94 MeV [2]. This new compact accelerator shows great application potential in inertial confinement fusion [3], warm dense matter generation [4,5], material science [6,7], imaging [8], fusion plasma diagnosis [9], and cancer treatment [10]. The most robust laser ion acceleration mechanism called target normal sheath acceleration (TNSA) method produces an electrostatic sheath field upward of 10^{12} V/m that ionizes the surface atoms almost instantaneously, forming a few-nanometer-thick ion layer, with the electron sheath resembling a virtual cathode [11,12]. The accelerated protons, which originate primarily from contaminant layers of water vapor or hydrocarbons on the target surface, have an exponentially decaying energy spectrum and a divergence

angle of around 10° [13]. Meanwhile, the emission region of laser-driven proton beam is mostly a few to tens of micrometers [1].

The construction of the transmission line for laser accelerators is also underway [14–17]. The phase space distribution of the beam is the basis for the design of the beamline, and the emittance is the key parameter describing the phase space distribution.

The emittance is a measure derived from the beam distribution in phase space that quantifies its divergence and ability to be focused. The normalized root mean square (rms) emittance of a particle beam is derived in the phase space (x, p_x) following Floettmann [18] as

$$\begin{aligned}\varepsilon_{n,\text{rms}} &= \frac{1}{m_0 c} \sqrt{\langle x^2 \rangle \langle p_x^2 \rangle - \langle x p_x \rangle^2} \\ &= \sqrt{\langle x^2 \rangle \langle \beta^2 \gamma^2 x'^2 \rangle - \langle x \beta \gamma x' \rangle^2},\end{aligned}\quad (1)$$

where $\beta = v/c$ is the velocity normalized to the speed of light, $\beta = v/c$ is the velocity relativistic factor, $x' = p_x/p_z$ is the rms divergence angle, p_x and p_z are the transverse momentum and the transport momentum, respectively, m_0 is the rest mass, and $\langle \dots \rangle$ denotes the average of the distribution. The area of the phase space ellipse is related to the normalized rms emittance $\varepsilon_{n,\text{rms}}$. In this manuscript, we use ε to represent $\varepsilon_{n,\text{rms}}$ and “emittance growth” is

*lc0812@pku.edu.cn

Published by the American Physical Society under the terms of the *Creative Commons Attribution 4.0 International* license. Further distribution of this work must maintain attribution to the author(s) and the published article’s title, journal citation, and DOI.

shorthand for “normalized rms emittance growth” for convenience. A beam with smaller emittance can be transported to an aiming area with lower pipe dimensions and a lower magnetic field gradient. In the case of a proton beam (at the MeV level), the relativistic effect, i.e., $\gamma = 1$, can be simplified. Furthermore, for laser-driven proton beam, the space charge force can be neglected after a drift of millimeter-level distance [19,20]. So according to Eq. (1), after ignoring the coupling between energy and transverse angle, the emittance can be expressed as

$$\varepsilon^2 = (\langle\beta^2\rangle - \langle\beta\rangle^2)\langle x^2\rangle\langle x'^2\rangle + \varepsilon_0^2. \quad (2)$$

Here, the lower right corner mark 0 represents the parameter at the initial point, and the original rms emittance is defined as

$$\varepsilon_0^2 = \langle\beta\rangle^2(\langle x_0^2\rangle\langle x_0'^2\rangle - \langle x_0x_0'\rangle^2). \quad (3)$$

Due to fixed β , the emittance of quasimonoenergetic particles from traditional accelerators remains constant during drift, namely, $\varepsilon = \varepsilon_0$. But it does not hold for laser accelerated beams with a significant energy spread [26], where the relativistic factor variance term $(\langle\beta^2\rangle - \langle\beta\rangle^2)$ play an important role. In this manuscript, we mainly focus on the emittance growth ($\Delta\varepsilon = \sqrt{\varepsilon^2 - \varepsilon_0^2} = \sqrt{(\langle\beta^2\rangle - \langle\beta\rangle^2)\langle x^2\rangle\langle x'^2\rangle}$). The source size of a laser-driven proton beam is on the order of a micrometer and can be ignored, so for drift space, $x = x_0 + x_0'L \approx x_0'L = x'L$, in which the L is the transport distance, and x' is equal to the primary divergence at the target position, then

$$\Delta\varepsilon^2 = (\langle\beta^2\rangle - \langle\beta\rangle^2)L^2\langle x'^2\rangle^2. \quad (4)$$

We can see that, under the action of velocity dispersion and divergence angle, the emittance will increase rapidly with the transport distance. It indicates that unless the beam is only transmitted through a very short distance or with a selected narrow energy bandwidth, the advantage of small emittance of laser-accelerated proton beam may no longer exist.

In this manuscript, a practical estimation formula related to emittance growth to energy spread and divergence of laser-accelerated proton beam has been derived, which is consistent well with the simulation and experimental results. First, we have summarized the previous experiments of laser-accelerated proton beam emittance measurement. Some regulations on the increase of the emittance have been shown by the data. Then, we have derived the emittance growth formula under different energy spectrum distributions, which latter is extended from drift space to a beamline with a focusing component. It is found that when the original emittance can be ignored, the emittance growth value is verified to be proportional to the energy spread and the quadratic power of the divergence angle. The proper beam transmission and control is one of the core parts to realize the application of laser accelerator. With this formula, the emittance growth under arbitrary parameters (energy spread, divergence, central energy, and drift length) can be quickly predicted, helping the matching of any beamline component and the beams. This is of great significance to the laser-driven proton beam line design.

II. EXPERIMENTS OF EMITTANCE MEASUREMENT

Figure 1 is a summary of the published emittance measurement results of the laser accelerated proton beam. The rear surface of the target ($z = 0$), the black hollow

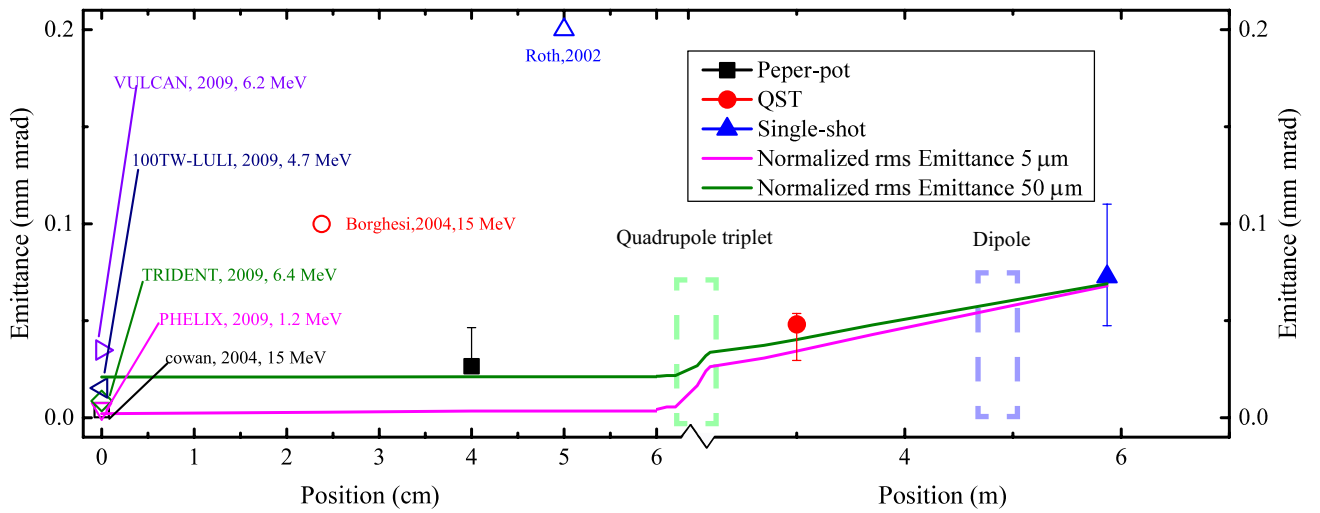


FIG. 1. Summary of the laser accelerated proton beam emittance measurements. Solid lines are the emittance evolution during transport in simulations. Solid points with error bars are CLAPA experimental results [21,22]. Hollow points without errorbar show the maximum emittance measurement result reported at different positions of each system [11,23–25].

square point shows a <0.004 mm mrad measured by the proton imaging of the microstructure target [11]. This is recognized as the initial emittance of the laser accelerated proton beam. The other hollow points are the measured emittance for different laser experimental systems by the microstructure target. The emittance varies at different laser experimental systems [23] but does not exceed 0.05 mm mrad at the source point. A few centimeters away from the target, by using slits [24] or meshes [25] placed in the ion beam path, the normalized emittance is between 0.1 and 0.2 mm mrad, as shown by the red hollow symbol and the blue hollow triangle symbol. The above measurement is based on a full beam. We can see that without constraints the emittance increases rapidly in the free drift space.

The emittance variation of the laser-driven accelerated ion beam in a beamline [22] was first measured at the Compact LAsER Plasma Accelerator (CLAPA) [16,27,28] at Peking University. The protons were primarily focused by a quadrupole triplet electromagnet, whose first quadrupole is located at 19 cm behind the target, and then energy dispersed by a 45° dipole magnet placed 3.57 m behind the triplet. The positions of the magnets are shown in Fig. 1 with dotted lines. Only those protons with divergence smaller than ± 20 mrad (corresponding to rms divergence of about $x'_0 \approx 8.4$ mrad) were input to the beamline in the emittance measurement experiment to avoid the effect of transverse nonlinearity in applied forces of magnets on the result. The experiment results are shown by the symbols with error bars. The solid black square symbol is the emittance measured using pepperpot method [29] at 4 cm after the target, which is <0.02 mm mrad. This value is significantly lower than previous measurements [24,25] because the proton beam angle is limited to $x'_0 \approx 8.2$ mrad. The solid red circle symbol is the measurement at 2.5 m after the quadrupole triplet by quadrupole scan technique, which is $0.048^{+0.006}_{-0.018}$ mm mrad. The solid blue triangle symbol is the result at 1.3 m after the dipole by single-shot emittance measurement [30], which is $0.073^{+0.037}_{-0.026}$ mm mrad. The solid lines in this figure are simulation results based on CLAPA parameters, where the source sizes of the beam are 5 and 50 μm , for pink and green lines, respectively.

From Fig. 1, it can be seen that the emittance is closely related to the experimental parameters and the beam measurement methods. However, an increasing trend with transmission distance is clear. It also indicate that compare to $\Delta\epsilon$, the initial emittance is small enough and can be ignored. As the energy chromatic aberration is the main factor causing the deterioration of the emittance, in the next section, we will quantify the emittance growth effect under various energy spectrum distributions.

III. EMITTANCE GROWTH OF LASER-ACCELERATED PROTON BEAM

Reviewing Eq. (4), it is necessary to establish the relationship between the relativistic factor variance term

and the beam energy distribution (for instance, the energy spread). Here, we defined the definition of relative energy spread (δ_E) as follows:

$$\delta_E^2 = \frac{\langle E_k^2 \rangle - \langle E_k \rangle^2}{\langle E_k \rangle^2} = \frac{\langle v^4 \rangle - \langle v^2 \rangle^2}{\langle v^2 \rangle^2}, \quad (5)$$

where E_k is the kinetic energy of charged particles. Eq. (5) establishes the relationship between the variance and energy spread of relativistic factors.

Let us first assume a most general case where the velocity of the proton beam is Gaussian distribution $f(v) = \frac{1}{\sqrt{2\pi}\delta} e^{-\frac{(v-\bar{v})^2}{2\delta^2}}$, where \bar{v} and δ are the average velocity and the variance of velocity, respectively. The statistical values of the velocity distribution are

$$\begin{aligned} \langle v \rangle &= \bar{v}, \\ \langle v^2 \rangle &= \bar{v}^2 + \delta^2, \\ \langle v^4 \rangle &= 3\delta^4 + 6\bar{v}^2\delta^2 + \bar{v}^4. \end{aligned} \quad (6)$$

Substituting Eq. (6) into Eq. (5), the energy spread can be expressed as

$$\delta_E^2 = 2 - \frac{2\bar{v}^4}{(\bar{v}^2 + \delta^2)^2}. \quad (7)$$

After simplifications, for Gaussian velocity distribution, the variance of relativistic factor is written as a function of energy spread:

$$\langle \beta^2 \rangle - \langle \beta \rangle^2 = \frac{\delta^2}{c^2} = \beta_0^2 \left(\sqrt{\frac{1}{1 - \frac{\delta_E^2}{2}}} - 1 \right), \quad (8)$$

in which $\beta_0 = v_0/c$, v_0 is the average value of speed. Based on the above derivation, Eq. (4) becomes

$$\Delta\epsilon^2 = \beta_0^2 \left(\sqrt{\frac{1}{1 - \frac{\delta_E^2}{2}}} - 1 \right) L^2 \langle x'^2 \rangle. \quad (9)$$

When δ_E is small ($<30\%$), the emittance growth formula tends to the approximate formula of low energy dispersion for Gaussian velocity distribution

$$\Delta\epsilon = \beta_0 \left(\frac{\delta_E}{2} \right) L x_0'^2. \quad (10)$$

Through the same process, we can derive the expression of the emittance of proton beams for different distributions, as illustrated in Table I. Both velocity distribution (easier to obtain analytical solution) and energy distribution (more commonly used in experiments and easy to measure) are considered. We also calculate the truncated exponential

TABLE I. Emittance growth formula of different distributions.

Spectrum distribution	Distribution equation	Emittance growth formula
Gaussian velocity distribution	$f(v) = \frac{1}{\sqrt{2\pi}\delta} e^{-\frac{(v-\bar{v})^2}{2\delta^2}}$	$\varepsilon^2 = \beta_0^2 \left(\sqrt{\frac{1}{1-\frac{\delta_E^2}{E^2}}} - 1 \right) L^2 \langle x'^2 \rangle^2 + \varepsilon_0^2$
Uniform velocity distribution	$f(v) = \begin{cases} \frac{1}{2\delta\bar{v}}, & v \in (\bar{v} - \bar{v}\delta, \bar{v} + \bar{v}\delta) \\ 0, & \text{other} \end{cases}$	$\varepsilon^2 = -\beta_0^2 \left(\frac{10-5\delta_E^2-2\sqrt{5(5-4\delta_E^2)}}{5\delta_E^2-4} \right) L^2 \langle x'^2 \rangle^2 + \varepsilon_0^2$
Gaussian energy distribution	$f(E) = \frac{1}{\sqrt{2\pi}\delta_0} e^{-\frac{(E-\bar{E})^2}{2\delta_0^2}}$	$\langle v \rangle = \int_0^{\bar{v}} \sqrt{\frac{2}{\pi}} \frac{mv^2}{\delta_E E} e^{-\frac{m^2}{8(\delta_E \bar{E})^2}(v^2 - v_0^2)^2} dv$ $\langle v^2 \rangle = v_0^2$ $\langle v^4 \rangle = v_0^4 + \left(\frac{2\delta_E \bar{E}}{m} \right)^2$
Uniform energy distribution	$f(E) = \begin{cases} \frac{1}{2\delta\bar{E}}, & E \in (\bar{E} - \bar{E}\delta, \bar{E} + \bar{E}\delta) \\ 0, & \text{other} \end{cases}$	$\varepsilon^2 = \beta_0^2 \left(\frac{9\delta_E^2 + 2(1-3\delta_E^2)^{\frac{3}{2}} - 2}{27\delta_E^2} \right) L^2 \langle x'^2 \rangle^2 + \varepsilon_0^2$
Truncated exponential energy distribution	$f(E) = \begin{cases} \frac{N_0}{\bar{E}} e^{-\frac{E}{\bar{E}}}, & E \in (\bar{E} - \bar{E}\delta, \bar{E} + \bar{E}\delta) \\ 0, & \text{other} \end{cases}$	$\langle v \rangle = \int_{\bar{v}}^{\bar{v}\sqrt{1+\delta}} 2N_0 v e^{-\frac{mv^2}{2k_0 T}} dv$ $\langle v^2 \rangle = \int_{\bar{v}}^{\bar{v}\sqrt{1+\delta}} 2N_0 v e^{-\frac{mv^2}{2k_0 T}} dv$ $\langle v^4 \rangle = \int_{\bar{v}}^{\bar{v}\sqrt{1+\delta}} 2N_0 v^3 e^{-\frac{mv^2}{2k_0 T}} dv$

energy distribution, which is closest to the TNSA experimental measurement [16]. Most distributions can obtain formula expressions except for the Gaussian energy distribution and the truncated exponential energy distribution, which can still be solved numerically. More details of the derivation process can be seen in the Appendix.

Figure 2(a) is the emittance calculation results of the proton beam with a central energy of 5 MeV, a divergence angle of ± 20 mrad, after a drift length of 1 m. The initial emittance is set at 0.02 mm mrad. The red solid and dotted lines are the results of Gaussian velocity distribution and Gaussian energy distribution; the blue solid and dotted lines are the results of uniform velocity distribution and uniform energy distribution; the green dotted line is the result of truncated exponential energy distribution; and the black solid line is the result of Gaussian velocity distribution of low energy spread [as Eq. (10)]. The upward convexity of the truncated exponential distribution in Fig. 2(a) primarily arises from the fact that the weight and contribution of the low-energy proton increase as the energy spread increases. Therefore, the decrease in β resulted in a decrease in emittance growth.

Figure 2(b) is the corresponding relative deviation of different distributions from Eq. (10). It indicates that the emittance growth values are very consistent when the δ_E is less than 30%. Because the achromatic ability of current beamlines is less than 5% [15–17,31], Eq. (11) can be used as a universal calculation formula. What is more, the emittance growth is commonly several orders of magnitude larger than the initial emittance, so ignoring the original small emittance ε_0 , Eq. (10) can be rewritten as

$$\varepsilon = \beta_0 \left(\frac{\delta_E}{2} \right) L x_0'^2. \quad (11)$$

To intuitively display the relationship between the emittance growth and the initial parameters of the proton beam, we have made a series of parameter scanning. Figure 3 shows the variation of emittance growth of a proton beam with arbitrary central energy and drift length. The energy spread is fixed at 2% and divergence angle is 5.2 mrad (same as Ref [22]). Taking the result of Fig. 1 as an example, we drew two white dashed lines: the horizontal one presents a drift length of 2.85 m, which equals the space between the quadrupole and the dipole magnet in Fig. 1; the vertical one present that the energy of the proton is 5 MeV. The intersection of the two lines indicates that the emittance growth value is about 0.075 mm mrad.

Next, we will study the influence of beam emittance growth on beamline design. The central energy of the proton beam is 5 MeV, and the entrance of a beamline is set at 10 cm behind the proton source point. Figure 4 shows the emittance growth with different energy spread and divergence for the proton beam after a drift length of 0.1 m. Assuming the emittance acceptance capability of the beamline is 0.1 mm mrad (as the contour line in Fig. 4), we can find that the maximum acceptable divergence angle is about 10 mrad (star A) for protons with an energy spread of 20%, while it is about 40 mrad (star B) for protons with an energy spread of 1%. It indicates that to design a beamline for laser-accelerated protons, the aimed energy spectrum and the divergence angle must be compromised. Either way, the most of the laser-accelerated proton beam will be lost due to the failure of effective transport caused

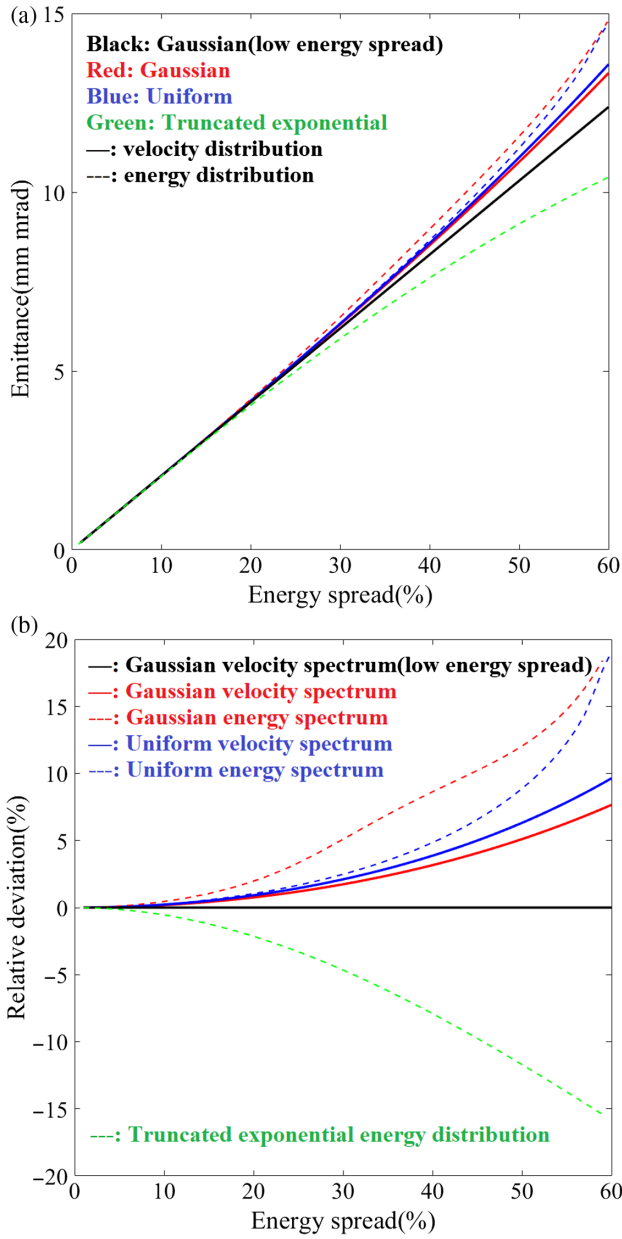


FIG. 2. (a) Emittance varies with energy spread, in which red is the Gaussian distribution, blue is the uniform distribution, green is the truncated exponential distribution, the solid line represents velocity spectrum distribution, the dotted line represents energy spectrum distribution, and the black solid line is the result of low energy spread approximate formula of Gaussian velocity spectrum. The simulation parameters of the proton beam are, respectively, the central energy of 5 MeV, the divergence of ± 20 mrad, the original emittance of 0.02 mm mrad, and the drift length of 1 m. (b) The relative deviation of different spreads compared with Eq. (10).

by the divergence angle of several hundred mrad and the nearly 100% energy dispersion. Therefore, it is preferable to make adjustments from the source, such as using concave target [32] to reduce the diverged angle, or using the laser radiation pressure dominated acceleration

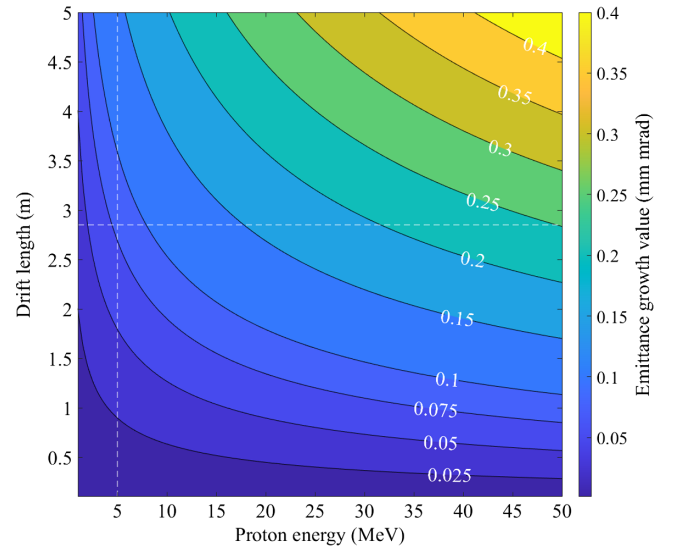


FIG. 3. Emittance growth values, calculated by Eq. (11), of proton beam with the energy spread of 2% and the divergence angle of 5.2 mrad with arbitrary central energy and drift length. The white dashed lines are the central energy of 5 MeV and the drift length of 2.85 m.

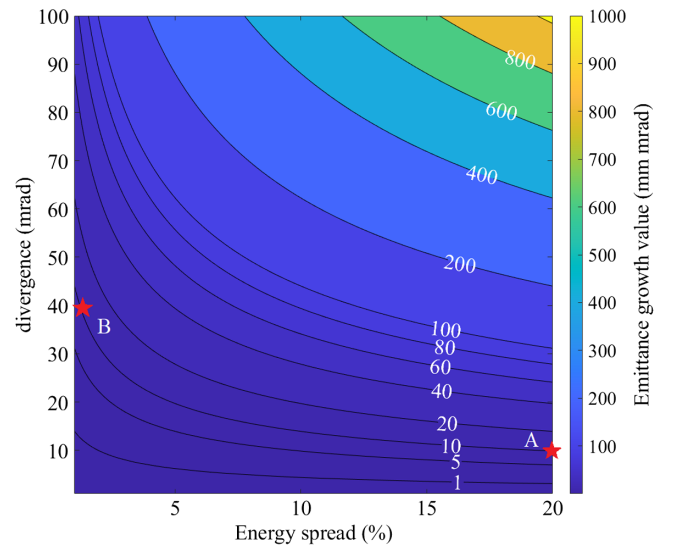


FIG. 4. Emittance growth values, calculated by Eq. (11), of the proton beam with the central energy of 5 MeV and the drift length of 0.1 m at energy spread of 0%–20% and divergence of 0–100 mrad. Stars A and B show a beamline with a maximum transported emittance of 10 mm mrad with an energy spread of 20% and 1%.

mechanisms [33] and postacceleration mechanisms [34] to compress the energy spectrum.

IV. EXTENSION OF EMITTANCE GROWTH FORMULA

The above analysis is focused on the drift space, and emittance growth with a beam-focusing element case

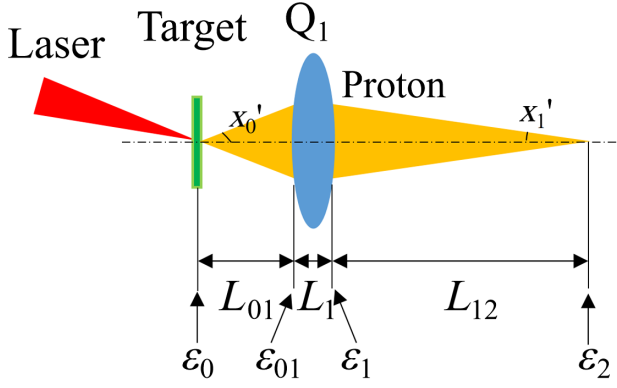


FIG. 5. DFD system, the subscripts 0, 01, 1, and 2 are, respectively, the target position, entrance of focus element, output of focus element, and detection position.

(drift + focus + drift, shorted as DFD system in this manuscript) is discussed in this section, as illustrated in Fig. 5. We first set the source size, divergence, and normalized rms emittance of a laser accelerated proton beam at the target position are x_0 , x_0' , and ϵ_0 . The focal length of a lens is actually coupled with the energy, and the x and x' of the protons at the focal point to be not independent of each other. As a result, Eq. (2) will not always hold. For a beam-focusing element, the focus length $f_x = \frac{1}{K_1 L_1}$, in which $K_1 = \frac{300}{\gamma \beta E_0 (\text{MeV})} \frac{\partial B_y}{\partial x}$, E_0 is the rest energy of particles, and $\frac{\partial B_y}{\partial x}$ is the magnetic field gradient. When the thin lens approximation condition ($\sqrt{K_1 L_1} \ll 1$) is satisfied, the transfer matrix of DFD system is

$$M_x = \begin{pmatrix} 1 - \frac{AL_{12}}{\beta} & L_{01} + L_{12} - \frac{AL_{01}L_{12}}{\beta} \\ -\frac{A}{\beta} & 1 - \frac{AL_{01}}{\beta} \end{pmatrix}, \quad (12)$$

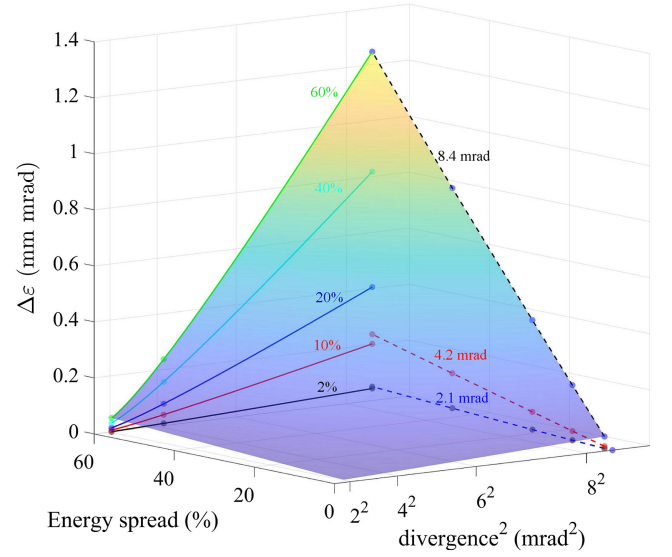


FIG. 6. CST simulation result of the emittance growth between the target and detection positions at CLAPA. The in-plane color scale represents the emittance growth value. Dashed lines represent the emittance growth of protons with different energy spreads, whose different colors represented different divergence angles [2.1 mrad (blue), 4.2 mrad (red), and 8.4 mrad (black)]. Lines represent the emittance growth of different divergence angles, whose different colors represented different energy spreads [2% (black), 10% (red), 20% (blue), 40% (blue-green), and 60% (green)].

in which $A = \frac{300L_1}{E_0 (\text{MeV})} \frac{\partial B_y}{\partial x}$ is a constant. Then $x_2 = (1 - \frac{AL_{12}}{\beta})x_0 + (L_{01} + L_{12} - \frac{AL_{01}L_{12}}{\beta})x_0'$, $x_2' = (\frac{-A}{\beta})x_0 + (1 - \frac{AL_{01}}{\beta})x_0'$. Ignoring the source size, the emittance growth from position 0 to position 2 is equal to the emittance at the position 2,

$$\Delta \epsilon_{02} = \epsilon_2 = \sqrt{\left\langle (\beta - AL_{01})^2 \right\rangle \left\langle \left(L_{01} + L_{12} - \frac{AL_{01}L_{12}}{\beta} \right)^2 \right\rangle - \left\langle (\beta - AL_{01}) \left(L_{01} + L_{12} - \frac{AL_{01}L_{12}}{\beta} \right) \right\rangle^2} \langle x_0'^2 \rangle. \quad (13)$$

For imaging system, $M_{12} = L_{01} + L_{12} - \frac{AL_{01}L_{12}}{\beta} = 0$. When the energy spread is small,

$$L_{01} + L_{12} - \frac{AL_{01}L_{12}}{\beta} = L_{01} + L_{12} - \frac{AL_{01}L_{12}}{\beta_0} \left(\frac{1}{1 - \frac{\beta_0 - \beta}{\beta_0}} \right) \approx \frac{AL_{01}L_{12}(\beta - \beta_0)}{\beta_0^2}, \quad (14)$$

then the $\Delta \epsilon_{02}$ can be expressed as

$$\begin{aligned} \Delta \epsilon_{02} &= \sqrt{\left\langle (\beta - AL_{01})^2 \right\rangle \left\langle \left(\frac{AL_{01}L_{12}(\beta - \beta_0)}{\beta_0^2} \right)^2 \right\rangle - \left\langle (\beta - AL_{01}) \left(\frac{AL_{01}L_{12}(\beta - \beta_0)}{\beta_0^2} \right) \right\rangle^2} \langle x_0'^2 \rangle \\ &= \frac{AL_{01}L_{12}(\beta_0 - AL_{01})}{\beta_0^2} \sqrt{\langle \beta^2 \rangle - \langle \beta \rangle^2} \langle x_0'^2 \rangle = \frac{AL_{01}L_{12}(\beta_0 - AL_{01})}{\beta_0} \left(\frac{\delta_E}{2} \right) \langle x_0'^2 \rangle = AL_{01}^2 \left(\frac{\delta_E}{2} \right) \langle x_0'^2 \rangle. \end{aligned} \quad (15)$$

This paragraph discusses the coupling effect between the focal length of a focusing element and the energy of particles in a DFD system. This proportional relationship is convinced by the CST simulation of CLAPA beam line [27]. For the vertical direction, the CLAPA beam line can be approximated as a DFD system. Protons with source size of 50 μm and divergence of ± 2.1 mrad (blue dashed line), ± 4.2 mrad (red dash line), and ± 8.4 mrad (black dashed line) were simulated. The $\Delta\varepsilon$ between the target position and the detection position (1.3 m after the dipole, corresponding to the blue point in Fig. 1) is shown as Fig. 6, in which the coefficient of determination value of linear fitting for each line is better than 0.999, verifying that $\Delta\varepsilon \propto \delta_E$. The line of Fig. 6 shows the emittance growth of protons with different divergence angles and energy spread of 2% (black line), 10% (red line), 20% (blue line), 40% (blue-green line), and 60% (green line) during transportation, the abscissa axis is the square of divergence, which shows $\Delta\varepsilon \propto x_0^2$.

V. CONCLUSIONS

Particle emittance is one of the most important parameters for a beamline. The wide energy spread of laser protons will cause the dispersion of the rotated velocity of the phase space ellipse and lead to an emittance growth term, which is related to focal length, transport length, relative energy spread, and divergence angle. The emittance growth prediction formula with different distributions at drift space and extension formula at the DFD system is qualitatively verified by CST simulation and quantitatively verified by experiment. When the original emittance can be ignored, the emittance growth value is verified to be proportional to the energy spread and the quadratic power of the divergence angle at any part for a laser-driven proton beamline. These formulas and proportional relationships can be used for emittance prediction and monitoring, which is of great significance for laser-driven proton beam line upgrade and design.

ACKNOWLEDGMENTS

This work was supported by the National Natural Science Foundation of China (Grant No. 12205007, No. 11921006, and No. 12122501) and the National Grand Instrument Project (No. 2019YFF01014400 and No. 2019YFF01014404).

APPENDIX: EMITTANCE GROWTH DERIVATION PROCESS

1. Uniform distribution of velocity

For the beam with uniform velocity distribution, a central velocity is assumed to be v_0 , a distribution domain radius is $v_0\delta$, and the probability density distribution satisfies the formula (A1):

$$f(v) = \begin{cases} \frac{1}{2\delta v_0}, & v \in (v_0 - v_0\delta, v_0 + v_0\delta) \\ 0, & \text{other.} \end{cases} \quad (\text{A1})$$

The variance term of the relativistic factor $\langle\beta^2\rangle - \langle\beta\rangle^2 = \frac{\langle v^2\rangle - \langle v\rangle^2}{c^2} = \frac{\delta^2 v_0^2}{3}$. The expectation of speed, the second and fourth power of speed is

$$\begin{aligned} \langle v \rangle &= v_0, \\ \langle v^2 \rangle &= v_0^2 + \frac{\delta^2 v_0^2}{3}, \\ \langle v^4 \rangle &= \frac{\delta^4 v_0^4}{5} + 2v_0^4 \delta^2 + v_0^4. \end{aligned} \quad (\text{A2})$$

Then, the energy spread can be written as a function of the variance of relativistic factors:

$$\delta_E^2 = \frac{\langle v^4 \rangle - \langle v^2 \rangle^2}{\langle v^2 \rangle^2} = \frac{\frac{4}{45} \frac{\delta^4 v_0^4}{c^4} + \frac{4}{3} \frac{v_0^4 \delta^2}{c^2 c^2}}{\left(\frac{v_0^2}{c^2} + \frac{\delta^2 v_0^2}{3c^2}\right)^2} = \frac{\frac{4}{45} \delta^4 + \frac{4}{3} \delta^2}{\left(1 + \frac{\delta^2}{3}\right)^2}. \quad (\text{A3})$$

The beam emittance equation with uniform velocity distribution is obtained as

$$\varepsilon^2 = -\beta_0^2 \left(\frac{10 - 5\delta_E^2 - 2\sqrt{5(5 - 4\delta_E^2)}}{5\delta_E^2 - 4} \right) L^2 \langle x'^2 \rangle + \varepsilon_0^2. \quad (\text{A4})$$

2. Gaussian distribution of energy

The traditional TNSA energy spectrum can be obtained by the superposition of multiple Gaussian distributions. Therefore, the emittance growth of the Gaussian distribution energy spectrum is deduced here. When the proton beam energy spectrum satisfies $f(E) = \frac{1}{\sqrt{2\pi}\delta_0} e^{-\frac{(E-E_0)^2}{2\delta_0^2}}$. It is equivalent to that the square of velocity is Gaussian distribution, and the average velocity is $v_0 = \sqrt{2E_0}/m$, in which the absolute energy spread is δ_0 , and the relative energy spread is δ_E , which defined as $\delta_0 = \delta_E E_0$. According to the distribution theorem of the function of a one-dimensional continuous random variable in probability statistics, the calculated velocity distribution function is

$$\begin{aligned} f_Y(v) &= f(1/2mv^2) |(1/2mv^2)'|, \quad v \in (0, +\infty), \\ &= \frac{\sqrt{1}}{\sqrt{2\pi}\delta_E E_0} e^{-\frac{(1/2mv^2 - 1/2mv_0^2)^2}{2(\delta_E E_0)^2}} mv, \quad v \in (0, +\infty), \\ &= \sqrt{\frac{1}{2\pi}\frac{mv}{\delta_E E_0}} e^{-\frac{m^2}{2(\delta_E E_0)^2}(v^2 - v_0^2)^2}, \quad v \in (0, +\infty). \end{aligned} \quad (\text{A5})$$

The integration of (A5) is relatively cumbersome, but from the symmetry of the distribution function, the

expectation of speed is $v_0 = \sqrt{2E/m}$, the expectation of the square of the velocity and the expectation of the fourth power of velocity can be obtained directly by using the properties of continuous distribution variance and expectation:

$$\begin{aligned}\langle v^2 \rangle &= \langle 2E/m \rangle = E_0/2m = v_0^2, \\ \langle v^4 \rangle &= v_0^4 + \left(\frac{2\delta E E_0}{m}\right)^2.\end{aligned}\quad (\text{A6})$$

Then, the variance of relativistic factors $\langle \beta^2 \rangle - \langle \beta \rangle^2 = \frac{\langle v^2 \rangle - \langle v \rangle^2}{c^2}$. In which,

$$\begin{aligned}\langle v \rangle &= \int_0^{\text{inf}} v f_Y(v) dv \\ &= \int_0^{\text{inf}} \sqrt{\frac{2}{\pi}} \frac{m v^2}{\delta E E_0} e^{\frac{-m^2}{8(\delta E E_0)^2}(v^2 - v_0^2)^2} dv.\end{aligned}\quad (\text{A7})$$

There is no analytical solution for this integral, but it can be solved by numerical integration under specific beam parameters. After getting the $\langle v \rangle$, the variance of relativistic factors can be obtained, then the beam emittance equation with uniform energy distribution can be obtained.

3. Uniform distribution of energy

According to the simulation of Zhu *et al.* [16], the proton energy spectrum transmitted into the rear end of the CLAPA beam line meets the truncated exponential descent energy spectrum. As an approximate, the emittance growth formula under uniform energy distribution is derived here. The proton beam energy spectrum satisfies

$$f(E) = \begin{cases} \frac{1}{2\delta E_0}, & E \in (E_0 - E_0\delta, E_0 + E_0\delta) \\ 0, & \text{other.} \end{cases}\quad (\text{A8})$$

Same to the derivation of the Gaussian energy spectrum, the calculated velocity distribution function is

$$\begin{aligned}f_Y(v) &= f(1/2mv^2)|(1/2mv^2)'|, \\ &v \in (\sqrt{1-\delta}v_0, \sqrt{1+\delta}v_0) \\ &= \begin{cases} \frac{1}{2\delta v_0^2}, & v \in (\sqrt{1-\delta}v_0, \sqrt{1+\delta}v_0) \\ 0, & \text{other.} \end{cases}\end{aligned}\quad (\text{A9})$$

At this time, the quartic and quadratic speed and the expectation of speed are

$$\begin{aligned}\langle v \rangle &= \frac{v_0}{3\delta} [(1+\delta)^{\frac{3}{2}} - (1-\delta)^{\frac{3}{2}}], \\ \langle v^2 \rangle &= v_0^2, \\ \langle v^4 \rangle &= v_0^4 + \frac{\delta^2}{3} v_0^4.\end{aligned}\quad (\text{A10})$$

Then the energy spread $\delta_E^2 = \frac{\langle v^4 \rangle - \langle v \rangle^2}{\langle v^4 \rangle^2} = \frac{\delta^2}{3}$, that is, $\delta_E = \frac{\sqrt{3}}{3}\delta$. So the variance of relativistic factors $\langle \beta^2 \rangle - \langle \beta \rangle^2 = \frac{\langle v^2 \rangle - \langle v \rangle^2}{c^2} = \beta_0^2 \left(1 - \frac{2+6\delta^2-2(1-\delta^2)^{\frac{3}{2}}}{9\delta^2}\right)$. The variance of energy distribution $\delta = \sqrt{3}\delta_E$, then the relationship between relativistic factor variance and energy spread is obtained

$$\langle \beta^2 \rangle - \langle \beta \rangle^2 = \beta_0^2 \left(\frac{9\delta_E^2 + 2(1-3\delta_E^2)^{\frac{3}{2}} - 2}{27\delta_E^2} \right).\quad (\text{A11})$$

The emittance growth formula under the uniform energy spectrum is

$$\epsilon^2 = \beta_0^2 \left(\frac{9\delta_E^2 + 2(1-3\delta_E^2)^{\frac{3}{2}} - 2}{27\delta_E^2} \right) L^2 \langle x^2 \rangle^2 + \epsilon_0^2.\quad (\text{A12})$$

4. Truncated exponential distribution of energy

The energy spectrum of laser accelerated proton beam can be considered to meet the Boltzmann distribution [35,36]. The particle beam near the transmitted central energy is generally collected for a well-designed laser accelerator and finally for the laser accelerator. The proton beam energy spectrum in the beamline can be considered a truncated Boltzmann distribution. Assume that the beamline transmission center energy is E_0 , the transmissible energy spread range is $E_0\delta$, and the probability density distribution satisfies the formula (A13)

$$f(E) = \begin{cases} \frac{N_0}{E} e^{\frac{E}{k_0 T}}, & E \in (E_0 - E_0\delta, E_0 + E_0\delta) \\ 0, & \text{other.} \end{cases}\quad (\text{A13})$$

In which, N_0 is the factor related to the number of particles. In the statistical process, the integral value of the above formula will be used for normalization. $k_0 T$ is the electron temperature in MeV. According to the distribution theorem of the function of one-dimensional continuous random variables in probability and statistics, let $v_0 = \sqrt{2E_0/m}$, the distribution function of the calculated velocity is

$$\begin{aligned}f_Y(v) &= f(1/2mv^2)|(1/2mv^2)'|, \quad v \in (v_0\sqrt{1-\delta}, v_0\sqrt{1+\delta}) \\ &= \frac{N_0}{E} e^{\frac{E}{k_0 T}} m v, \quad v \in (v_0\sqrt{1-\delta}, v_0\sqrt{1+\delta}) \\ &= \frac{2N_0}{v} e^{\frac{-mv^2}{2k_0 T}}, \quad v \in (v_0\sqrt{1-\delta}, v_0\sqrt{1+\delta}).\end{aligned}\quad (\text{A14})$$

The variance term of relativistic factor, the expectation of velocity square, and the expectation of velocity quartic can be obtained by numerical integration:

$$\begin{aligned}\langle v \rangle &= \int_{v_0\sqrt{1-\delta}}^{v_0\sqrt{1+\delta}} v f_Y(v) dv = \int_{v_0\sqrt{1-\delta}}^{v_0\sqrt{1+\delta}} 2N_0 e^{-\frac{mv^2}{2k_0T}} dv, \\ \langle v^2 \rangle &= \int_{v_0\sqrt{1-\delta}}^{v_0\sqrt{1+\delta}} v^2 f_Y(v) dv = \int_{v_0\sqrt{1-\delta}}^{v_0\sqrt{1+\delta}} 2N_0 v e^{-\frac{mv^2}{2k_0T}} dv, \\ \langle v^4 \rangle &= \int_{v_0\sqrt{1-\delta}}^{v_0\sqrt{1+\delta}} v^4 f_Y(v) dv = \int_{v_0\sqrt{1-\delta}}^{v_0\sqrt{1+\delta}} 2N_0 v^3 e^{-\frac{mv^2}{2k_0T}} dv.\end{aligned}\tag{A15}$$

Finally, the relationship between energy spread and emittance growth of energy truncated exponential distribution can be obtained by numerical integration.

-
- [1] M. Roth and M. Schollmeier, [arXiv:1705.10569](https://arxiv.org/abs/1705.10569).
- [2] A. Higginson, R. Gray, M. King, R. Dance, S. Williamson, N. Butler, R. Wilson, R. Capdessus, C. Armstrong, J. Green *et al.*, *Nat. Commun.* **9**, 724 (2018).
- [3] M. Roth, T. E. Cowan, M. H. Key, S. P. Hatchett, C. Brown, W. Fountain, J. Johnson, D. M. Pennington, R. A. Snavely, S. C. Wilks *et al.*, *Phys. Rev. Lett.* **86**, 436 (2001).
- [4] A. B. Zylstra, J. A. Frenje, P. E. Grabowski, C. K. Li, G. W. Collins, P. Fitzsimmons, S. Glenzer, F. Graziani, S. B. Hansen, S. X. Hu *et al.*, *Phys. Rev. Lett.* **114**, 215002 (2015).
- [5] P. K. Patel, A. J. Mackinnon, M. H. Key, T. E. Cowan, M. E. Foord, M. Allen, D. F. Price, H. Ruhl, P. T. Springer, and R. Stephens, *Phys. Rev. Lett.* **91**, 125004 (2003).
- [6] M. Barberio, M. Scisciò, S. Vallières, F. Cardelli, S. Chen, G. Famulari, T. Gangolf, G. Revet, A. Schiavi, M. Senzacqua *et al.*, *Nat. Commun.* **9**, 372 (2018).
- [7] M. Barberio, M. Scisciò, S. Vallières, S. Veltri, A. Morabito, and P. Antici, *Sci. Rep.* **7**, 12522 (2017).
- [8] A. Y. Faenov, T. Pikuz, Y. Fukuda, M. Kando, H. Kotaki, T. Homma, K. Kawase, T. Kameshima, A. Pirozhkov, A. Yogo *et al.*, *Appl. Phys. Lett.* **95**, 101107 (2009).
- [9] X. Yang, Y. Chen, C. Lin, L. Wang, M. Xu, X. Wang, and C. Xiao, *Rev. Sci. Instrum.* **85**, 11E429 (2014).
- [10] S. Kraft, C. Richter, K. Zeil, M. Baumann, E. Beyreuther, S. Bock, M. Bussmann, T. Cowan, Y. Dammene, W. Enghardt *et al.*, *New J. Phys.* **12**, 085003 (2010).
- [11] T. E. Cowan, J. Fuchs, H. Ruhl, A. Kemp, P. Audebert, M. Roth, R. Stephens, I. Barton, A. Blazevic, E. Brambrink *et al.*, *Phys. Rev. Lett.* **92**, 204801 (2004).
- [12] A. Macchi, M. Borghesi, and M. Passoni, *Rev. Mod. Phys.* **85**, 751 (2013).
- [13] Y.-X. Geng, Q. Liao, Y.-R. Shou, J.-G. Zhu, X.-H. Xu, M.-J. Wu, P.-J. Wang, D.-Y. Li, T. Yang, R.-H. Hu, D.-H. Wang, Y.-Y. Zhao, W. Ma, H.-Y. Lu, C. Lin, and X.-Q. Yan, *Chin. Phys. Lett.* **35**, 092901 (2018).
- [14] S. Busold, D. Schumacher, C. Brabetz, D. Jahn, F. Kroll, O. Deppert, U. Schramm, T. E. Cowan, A. Blažević, V. Bagnoud *et al.*, *Sci. Rep.* **5**, 12459 (2015).
- [15] F. Romano, F. Schillaci, G. Cirrone, G. Cuttone, V. Scuderi, L. Allegra, A. Amato, A. Amico, G. Candiano, G. De Luca *et al.*, *Nucl. Instrum. Methods Phys. Res., Sect. A* **829**, 153 (2016).
- [16] J. G. Zhu *et al.*, *Phys. Rev. Accel. Beams* **22**, 061302 (2019).
- [17] K. D. Wang, K. Zhu, M. J. Easton, Y. J. Li, C. Lin, and X. Q. Yan, *Phys. Rev. Accel. Beams* **23**, 111302 (2020).
- [18] K. Floettmann, *Phys. Rev. ST Accel. Beams* **6**, 034202 (2003).
- [19] Z. Jungao, Z. Yuan, L. Meifu *et al.*, *High Power Laser Phys. Technol.* **35**, 021004 (2023).
- [20] J. G. Zhu, K. Zhu, L. Tao, X. H. Xu, C. Lin, W. J. Ma, H. Y. Lu, Y. Y. Zhao, Y. R. Lu, and J. E. Chen, *Chin. Phys. C* **41**, 097001 (2017).
- [21] M. Wu, J. Zhu, D. Li, T. Yang, Q. Liao, Y. Geng, X. Xu, C. Li, Y. Shou, Y. Zhao, Y. Lu, H. Lu, W. Ma, C. Lin, K. Zhu, and X. Yan, *Nucl. Instrum. Methods Phys. Res., Sect. A* **955**, 163249 (2020).
- [22] M. J. Wu, D. Y. Li, J. G. Zhu, T. Yang, X. Y. Hu, Y. X. Geng, K. Zhu, M. J. Easton, Y. Y. Zhao, A. L. Zhang, H. Y. Lu, W. J. Ma, C. Lin, and X. Q. Yan, *Phys. Rev. Accel. Beams* **23**, 031302 (2020).
- [23] F. Nürnberg, M. Schollmeier, E. Brambrink, A. Blažević, D. Carroll, K. Flippo, D. Gautier, M. Geissel, K. Harres, B. Hegelich *et al.*, *Rev. Sci. Instrum.* **80**, 033301 (2009).
- [24] M. Roth, T. E. Cowan, J. Gauthier, J. M. Vehn, M. Allen, P. Audebert, A. Blazevic, E. Brambrink, J. Fuchs, M. Geissel *et al.*, *AIP Conf. Proc.* **650**, 485 (2002).
- [25] M. Borghesi, A. J. Mackinnon, D. H. Campbell, D. G. Hicks, S. Kar, P. K. Patel, D. Price, L. Romagnani, A. Schiavi, and O. Willi, *Phys. Rev. Lett.* **92**, 055003 (2004).
- [26] M. Migliorati, A. Bacci, C. Benedetti, E. Chiadroni, M. Ferrario, A. Mostacci, L. Palumbo, A. R. Rossi, L. Serafini, and P. Antici, *Phys. Rev. ST Accel. Beams* **16**, 011302 (2013).
- [27] J.-G. Zhu, K. Zhu, L. Tao, Y.-X. Geng, C. Lin, W.-J. Ma, H.-Y. Lu, Y.-Y. Zhao, Y.-R. Lu, J.-E. Chen *et al.*, *Chin. Phys. Lett.* **34**, 054101 (2017).
- [28] J. G. Zhu *et al.*, *Phys. Rev. Accel. Beams* **23**, 121304 (2020).
- [29] M. Zhang, Emittance formula for slits and pepper-pot measurement, Fermi National Accelerator Laboratory, Batavia, IL, Technical Report No. FNAL-TM-1988, 1996, https://inis.iaea.org/search/search.aspx?orig_q=RN:28018451.
- [30] S. K. Barber, J. van Tilborg, C. B. Schroeder, R. Lehe, H.-E. Tsai, K. K. Swanson, S. Steinke, K. Nakamura, C. G. R. Geddes, C. Benedetti *et al.*, *Phys. Rev. Lett.* **119**, 104801 (2017).
- [31] D. Jahn, D. Schumacher, C. Brabetz, J. Ding, S. Weih, F. Kroll, F. Brack, U. Schramm, A. Blažević, and M. Roth, *Nucl. Instrum. Methods Phys. Res., Sect. A* **909**, 173 (2018).
- [32] T. Okada, A. A. Andreev, Y. Mikado, and K. Okubo, *Phys. Rev. E* **74**, 026401 (2006).

-
- [33] T. Esirkepov, M. Borghesi, S. V. Bulanov, G. Mourou, and T. Tajima, *Phys. Rev. Lett.* **92**, 175003 (2004).
- [34] S. Kar, H. Ahmed, R. Prasad, M. Cerchez, S. Brauckmann, B. Aurand, G. Cantono, P. Hadjisolomou, C. L. Lewis, A. Macchi *et al.*, *Nat. Commun.* **7**, 10792 (2016).
- [35] M. Schollmeier, M. Geissel, A. B. Sefkow, and K. A. Flippo, *Rev. Sci. Instrum.* **85**, 043305 (2014).
- [36] F. Wagner, S. Bedacht, V. Bagnoud, O. Deppert, S. Geschwind, R. Jaeger, A. Ortner, A. Tebartz, B. Zielbauer, D. H. H. Hoffmann, and M. Roth, *Phys. Plasmas* **22**, 063110 (2015).